Synthesis O. Beyer et al. Paper

A Convenient Access to a [2]Rotaxane Proton Shuttle by Using a Fluorous Ponytail

Ole Beyer
Britta Hesseler
Ulrich Lüning*

Christian-Albrechts-Universität zu Kiel, Otto-Diels-Institut für Organische Chemie, Olshausenstraße 40, 24098 Kiel, Germany
luening@oc.uni-kiel.de

Dedicated to Professor Bernd Giese on the occasion of his 75th birthday

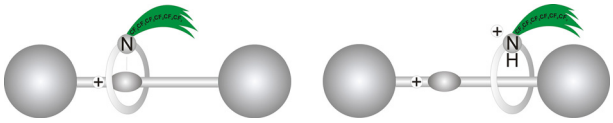

Received: 26.03.2015
Accepted after revision: 18.04.2015
Published online: 17.06.2015
DOI: 10.1055/s-0034-1380814; Art ID: ss-2015-t0202-op

Abstract The properties of rotaxanes and their constituents, ring and axle, sometimes do not differ much from one another resulting in tedious workup. In the case of a rotaxane designed to shuttle protons across a biological membrane (3–4 nm), molecular weight, shape, and functional groups of axle and rotaxane are similar. But when the macrocyclic ring of the rotaxane carries a fluorous residue, the fluorous effect distinguishes the rotaxane from the axle because the latter carries no fluorine atoms. This concept has been exploited to synthesize a [2]rotaxane in which the macrocyclic ring is protonable and the axle contains a permanent positive charge. Upon protonation/deprotonation of the macrocycle, a shuttling process is induced, which can lead to the transport of protons.

Key words rotaxane, trapping, macrocycles, proton transport, fluorine

The 'fuel' in cellular processes is adenosine triphosphate (ATP). It is synthesized by the enzyme ATPase from adenosine diphosphate (ADP) and phosphate.[1] This endergonic process is powered by a pH gradient. The pH gradient itself can be generated in different ways, for instance by metabolism of glucose. In contrast, halobacteria use light to build up a pH potential across the biological membrane.[2]

Molecular machines and motors try to mimic biological processes.[3] To mimic a light driven proton pumping process, a photoacid must be coupled with a transmembrane transporter. Attention has to be paid to the minute thickness of the biological membrane. The wavelengths of visible light (ca. 380–780 nm) are two orders of magnitude longer than the thickness of a biological membrane (3–4 nm). Therefore, light will always irradiate both sides of a biomembrane.

Photoacids are compounds which undergo an intramolecular reaction upon irradiation, resulting in an isomer with an increased acidity. A prototype is 2-nitrotoluene, which forms an *aci*-nitro derivative when irradiated,[4] and several derivatives thereof have been developed.[5] By placing such a photoacid on one side on the membrane, a pH gradient can be generated by irradiation.

The last element for a proton pump is a proton carrier. It must have the following features: it must be located in the membrane spanning it from one water layer to the other, it must be protonable by the acidity which is generated by the irradiation; however, it shall not be too basic as the proton shall be released at the opposite side of the membrane, and last, the carrier must be able to cross the membrane but shall not leave it in order to avoid 'bleeding'.

Mechanically interlocked molecules (MIMs)[6] perfectly allow a restricted mobility. In a rotaxane,[7] the ring can move from one side of the rotaxane to the other but cannot leave the axle. Accordingly, we have devised a [2]rotaxane containing a protonable macrocyclic ring[8] to be used as a proton shuttle. The axle of the rotaxane is designed unsymmetrically with a permanent positive charge and a binding site for the macrocycle on the side from which the proton shall be taken up.

In the resting state, the macrocycle is bound to the binding site. When a proton is delivered from this side [by a low pH (passive transport), or by use of a photoacid (active transport)], the macrocycle becomes protonated. The permanent positive charge in the axle repels the protonated macrocycle, which moves to the opposite end of the rotaxane. There, the proton can be released. If the rotaxane spans a membrane this process of uptake of a proton on one side and release on the opposite side of the membrane has allowed the transport of proton across a lipophilic membrane. When this process was propeled by the use of a photoacid, a pH gradient will be formed.

For the first realization of a [2]rotaxane proton shuttle of this design,[8] the following elements were incorporated: the protonable macrocycle contained a 2,6-disubstituted pyridine, the binding site for the macrocycle was an amide

group, and the permanent positive charge was introduced in form of a pyridinium ion. The rotaxane itself was synthesized using the trapping method. In this case, the copper-catalyzed 1,3-dipolar cycloaddition of an azide to an alkyne ('click' reaction) was used because copper coordinates to the pyridine unit of the macrocycle.[9]

Several [2]rotaxanes were synthesized but the yields were not satisfactory.[10] A major problem was the separation of the desired [2]rotaxane from the free axle, which is also formed in the synthesis. Although free axle and rotaxane differ by the macrocycle, they are still too similar. Therefore, we have changed the nature of the macrocycle by introduction of a fluorinated residue.

When fluorine atoms are present, interactions between molecules are drastically changed.[11] Fluorinated molecules behave different than other (nonfluorous) molecules, different than polar and also unpolar ones. When the extent of fluorination is high, even separate phases are formed, and the fluorous effect has been exploited in multilayer systems of immiscible liquids.[12] But also in compounds with a lower degree of fluorination, the fluorine content alters the nature of a molecule sufficiently to allow easier workup, for instance by extraction, or by chromatography with fluorinated phases.[11] Therefore, a fluorous 'ponytail' was attached to the macrocycle of a [2]rotaxane proton shuttle[8] as depicted in Figure 1.

In the previous proton shuttles,[8,10] the pyridine ring of the macrocycle was 4-methoxy substituted. In order not to influence the pyridine ring and its basicity too much, we decided to use a perfluoroalkylethoxy substituent, in particular the perfluorohexylethoxy residue because the respective iodide and the respective alcohol are commercially available. The chosen ponytail possesses two methylene groups as spacer, which isolates any influence of the fluorous residue from the pyridine and for instance its basicity.

The fluorous ponytail was introduced into the 29-membered pyridine macrocycle **9** in a nine-step synthesis. Chelidamic acid (**1**) and its ethyl ester **2** were prepared according to literature procedures.[13,14] To connect the fluorous ponytail to the hydroxyl group of chelidamic ester **2**, two ether forming reactions were tested: a Mitsunobu reaction with a fluorous alcohol and a Williamson ether synthesis with a

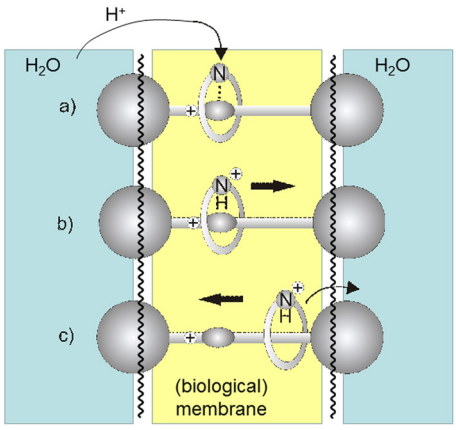

Figure 1 Mode of operation of a transmembrane proton shuttle based on a [2]rotaxane: a) In the resting state, the macrocycle is bound to a binding site next to a permanent positive charge. From this side a proton is delivered. b) The macrocycle becomes protonated and is repelled by the permanent positive charge in the axle. c) Once the protonated macrocycle reaches the other end of the rotaxane, the proton can be released, and the deprotonated macrocycle will diffuse back to the binding site.

fluorous iodide. Due to the low yields of the Mitsunobu reaction, the Williamson ether synthesis was preferred. But also in this reaction, the conditions had to be optimized. The combination of silver carbonate as base with toluene as solvent led to the best yield of fluorous ester **3** (93%), whereas standard conditions for Williamson ether synthesis led to no product at all. Fluorous diester **3** was then reduced with sodium borohydride to yield fluorous diol **4** in 90% yield. Next, **4** was brominated with phosphorus tribromide to give 84% of fluorous dibromide **5** (Scheme 1).

Starting from fluorous dibromide **5**, macrocycle precursor **7** could be obtained by a double Williamson ether synthesis with literature known benzyl alcohol **6**.[15] First, sodium hydride was used as base but the ether synthesis only gave 5% of the desired diene **7**. The low yield could be traced back to elimination reactions at the fluorous ponytail. By mass spectrometry, elimination of hydrogen fluoride and removal of the whole fluorous ponytail could be detected. Whether excess hydride anions or the sodium alcoholates attack the slightly acidic methylene group next to the fluo-

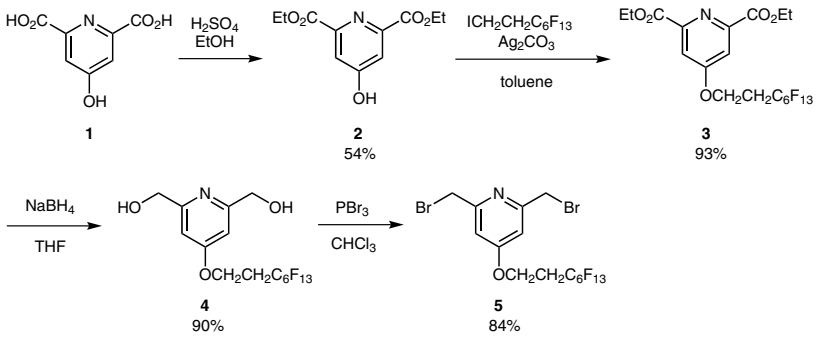

Scheme 1 Synthesis of fluorous dibromide **5**

rous residue has not been investigated, instead sterically demanding lithium diisopropylamide was chosen. Applying this base, the double Williamson ether synthesis led to 34% of isolated diene **7**.

Ring-closing metathesis of macrocycle precursor **7** using Grubbs' catalyst (1st generation) yielded unsaturated macrocycle **8** as a mixture of the *E*- and *Z*-isomers in 59% yield. Hydrogenation of this mixture using platinum(IV) oxide as catalyst gave the saturated fluorous macrocycle **9** in 75% yield (Scheme 2). Overall, 130 mg of the fluorous ring **9** was obtained in a total yield of 5%.

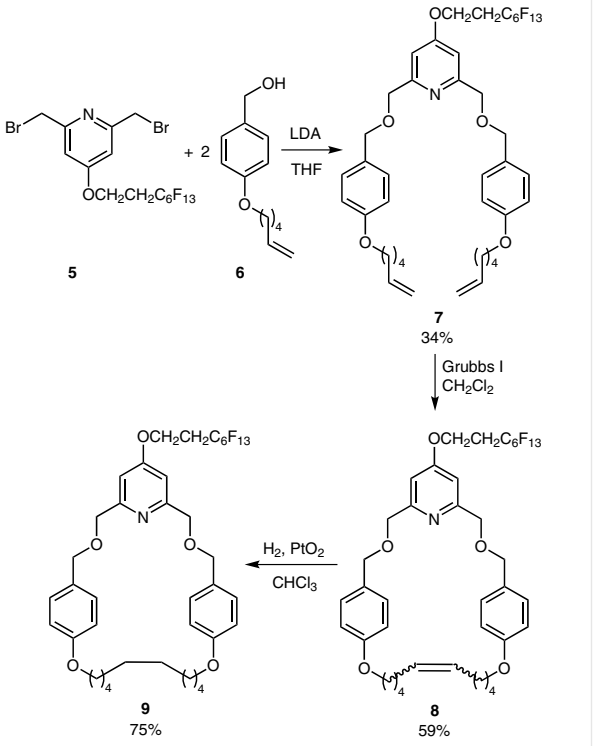

Scheme 2 Synthesis of fluorous macrocycle **9**

The synthesis of the envisaged fluorinated rotaxane **12** was carried out as developed for the nonfluorous analogue.[8] Cu(I)-catalyzed 1,3-dipolar cycloaddition ('click' reaction) of an alkyne half axle **10**[8] with an azide half axle **11**[8] was chosen to generate a triazole containing axle. Due to the coordination of the copper ions to the nitrogen atom of macrocycle **9**, the click reaction may take place inside the macrocycle thus producing the desired rotaxane **12** besides the free axle **13**. The copper ion simultaneously acts as catalyst for the 1,3-cycloaddition and as template to form the mechanically interlocked structure **12**. Therefore, copper had to be used in equimolar and not catalytic amounts. The desired fluorous rotaxane **12** was isolated in 14% yield (Scheme 3).

Although this yield of 14% is the highest yield so far for the synthesis of a rotaxane using the half axles **10** and **11**, the yield is comparably low with respect to related but smaller [2]rotaxanes, which have also been synthesized from simpler azide and alkyne half axles using the Cu(I)-catalyzed 1,3-cycloaddition. Leigh et al. were able to improve the yield of [2]rotaxane formation by using five equivalents of each half axle instead of only one equivalent.[16] But due to the longer and more time consuming syntheses of the half axles **10** and **11**, this approach was not chosen here because it would also produce more than 80% of free axle.

The structure of the fluorous rotaxane **12** was elucidated by different mass spectrometry and NMR spectroscopy experiments. MALDI-TOF spectrometry supplied a peak at m/z = 2520, which corresponds to the mass of the rotaxane **12** without its hexafluorophosphate counter ion. The elemental composition was confirmed by high resolution ion cyclotron mass spectrometry, which showed a signal for m/z = 1260.698. This corresponds to a protonated, doubly charged rotaxane **12** without the hexafluorophosphate counter ion.

A comparison of NMR spectra of rotaxane **12**, free axle **13**, and macrocycle **9** proved the structure of rotaxane **12** and furthermore determined the position of the macrocycle on the axle (Figure 2). The chemically induced upfield shifts of the pyridinium ion signals (3, 4, 5, 6) and signals 1, 2, and 7 of rotaxane **12** argue that the preferred position of the macrocycle is close to the pyridinium ion. Due to the aromatic rings of the macrocycle, the encapsulated part of the axle is shielded and the respective signals are shifted upfield. The position of macrocycle could also be confirmed by 2 D NOESY experiments, which showed cross signals between the aromatic protons c of macrocycle and signals 2, 3, 4, 5, and 6 of the axle. Two interactions may contribute to a preferred positioning of the macrocycle at this end of the axle: (i) formation of a hydrogen bond between the amide proton of the axle and the pyridine nitrogen atom of the macrocycle, and (ii) π–π-interactions between the aromatic rings of the macrocycle and the electron poor pyridinium ion of the axle.

But also other signals of the macrocyclic ring **9** support the rotaxane structure. The ^{1}H NMR spectrum of the symmetric macrocycle **9** shows one singlet each for the CH_2 groups $ArCH_2$ and $PyCH_2$. But in rotaxane **12**, these signals become more complex. Due to the unsymmetric axle, the macrocycle in rotaxane **12** is less symmetric. It possesses a front and a back side, and consequently the CH_2 singlets become pairs of doublets in rotaxane **12**.

The mechanically interlocked structure of rotaxane **12** was also proven by DOSY NMR experiments. The diffusion constant of a molecule is correlated with its solvodynamic radius, which depends on the size and shape of the molecule. Due to the smaller size of macrocycle **9** in comparison to axle **13** and rotaxane **12**, macrocycle **9** diffuses fastest

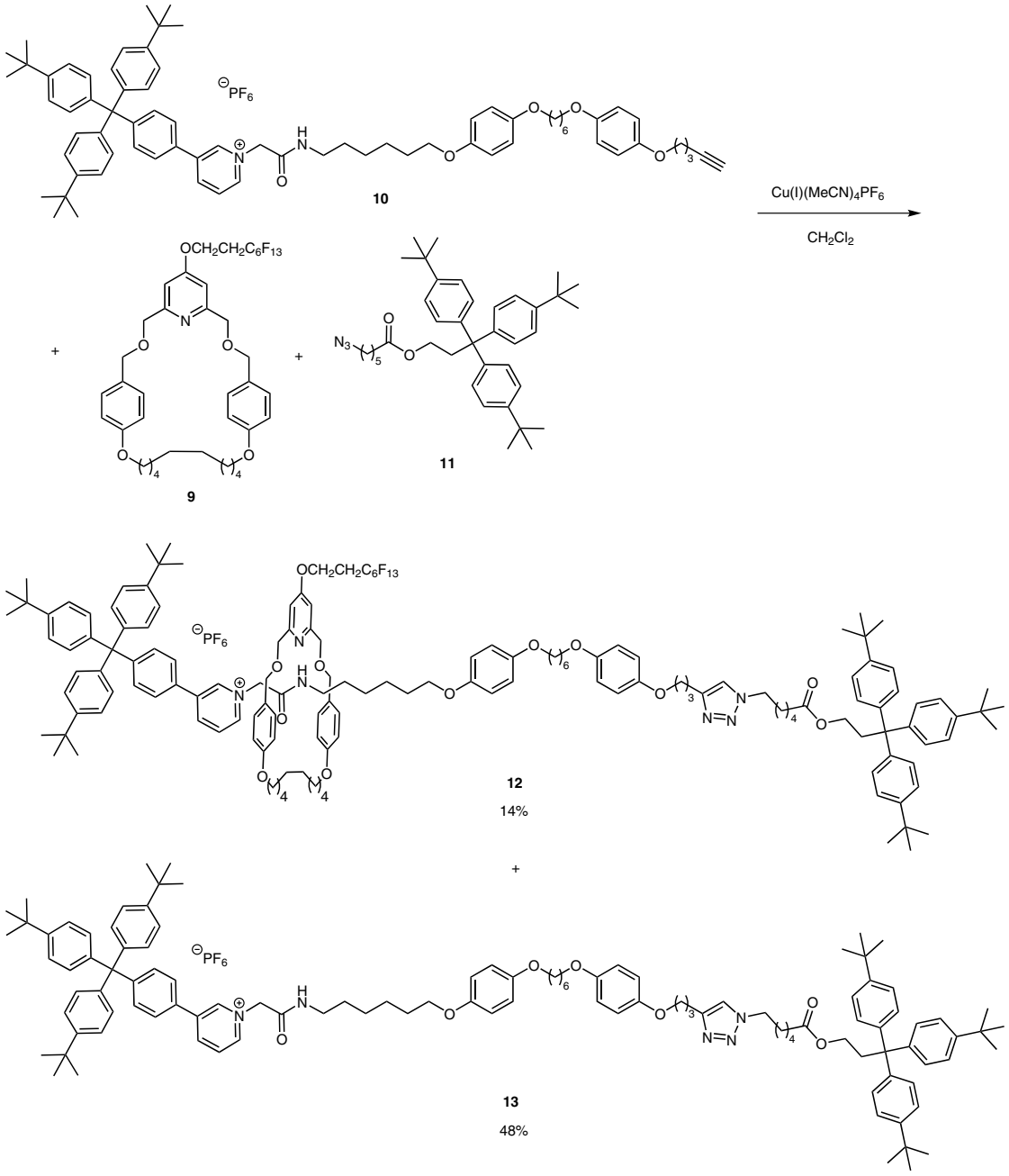

Scheme 3 Synthesis of fluorous rotaxane **12**

and therefore possesses the largest diffusion constant (Table 1). For rotaxane **12**, the diffusion constant derived from signals of ring protons is identical to the one obtained from protons of the axle giving additional evidence for the mechanical interlocking of axle and macrocyclic ring in rotaxane **12**. In a separate experiment, axle **13** and macrocycle **9** were mixed. Remarkably, the diffusion constant determined from ring protons in this mixture was different from free macrocycle **9** but also rotaxane **12**. This argues for supramolecular interactions between macrocycle **9** and axle **13** when they are mixed, probably the same interactions, which are responsible for the preferred position of the macrocycle close to the pyridinium unit of the axle in rotaxane **12**. A dynamic equilibrium between free axle **13** and free macrocycle **9** and such a supramolecular aggregate could explain the slightly smaller diffusion constant for macrocycle **9** in the mixture when compared to the free macrocycle.

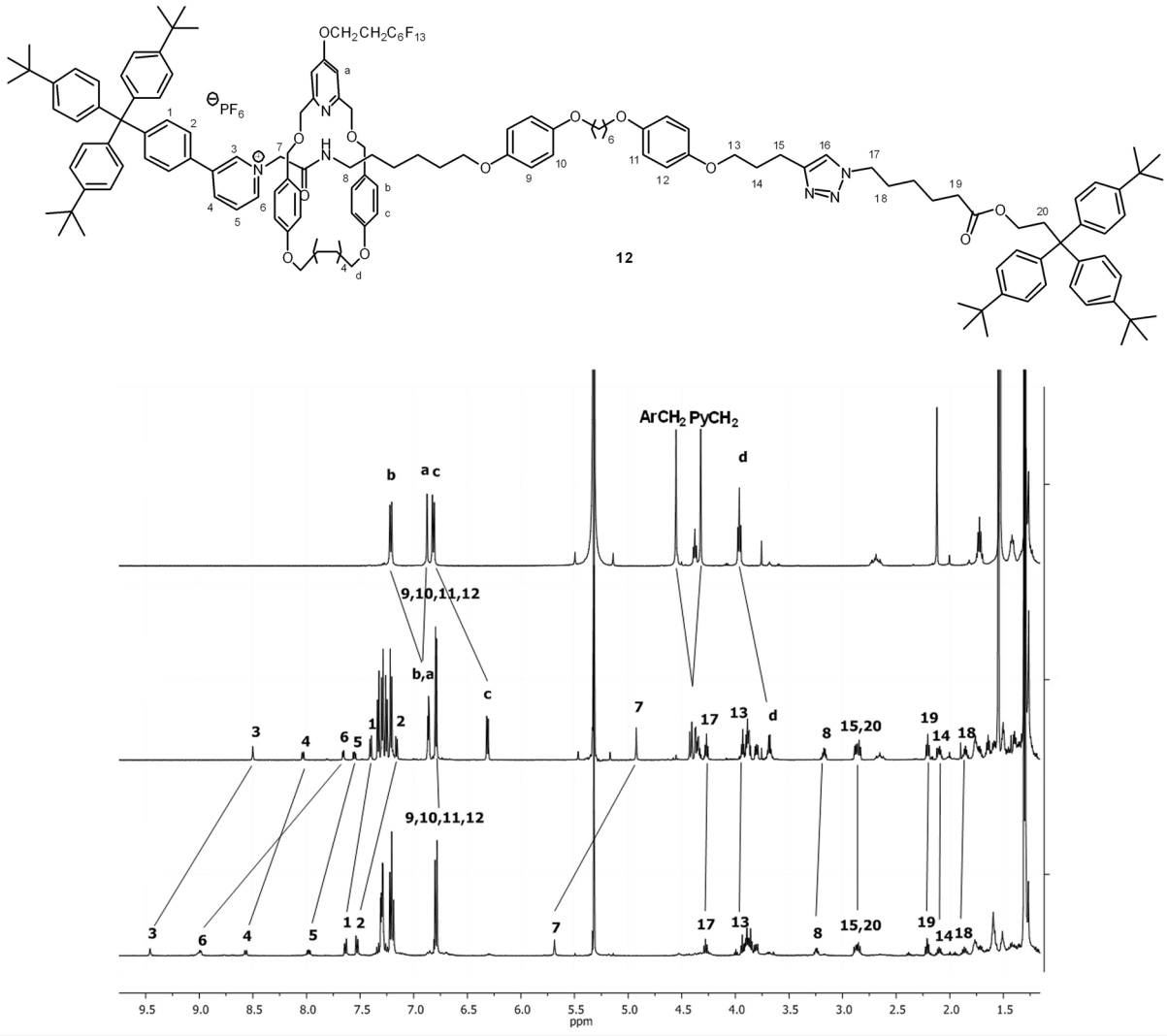

Figure 2 ^{1}H NMR spectra of free axle **13** (bottom), rotaxane **12** (middle), and macrocycle **9** (top) in CD_2Cl_2. Protons of the axle are numbered, protons of the macrocyclic ring are labeled with letters. Chemically induced shifts are indicated by solid lines.

Table 1 Diffusion Constants *D* at 298 K for Rotaxane **12**, its Components **13** and **9** and a Mixture of the Two Determined in CD_2Cl_2

	D [10^{-10} m^2s^{-1}] signals for	
	Axle	Macrocycle
Rotaxane **12**	4.67	4.64
Axle **13**	4.88	
Macrocycle **9**		9.35
Axle **13** + macrocycle **9**	4.59	7.38

When the diffusion constants (see Table 1) that were obtained from protons of the axle are compared for free axle **13** and rotaxane **12**, only small differences can be detected, indicating similar solvodynamic radii of rotaxane **12**, free axle **13**, and supramolecular aggregates of axle **13** and macrocycle **9**.

Finally, the ability of rotaxane **12** to transport a proton along the axle was investigated by ^{1}H NMR experiments. Difluoroacetic acid was chosen as proton source for two reasons. Its acidity is quite strong but in contrast to trifluoroacetic acid, its concentration can be determined in ^{1}H NMR spectra by integration. After addition of this acid to a solution of rotaxane **12**, the pyridine nitrogen atom of the macrocyclic ring became protonated. The repulsive interaction between the protonated, therefore positively charged macrocycle and the pyridinium cation of the axle led to a movement of the macrocycle along the axle (Scheme 4).

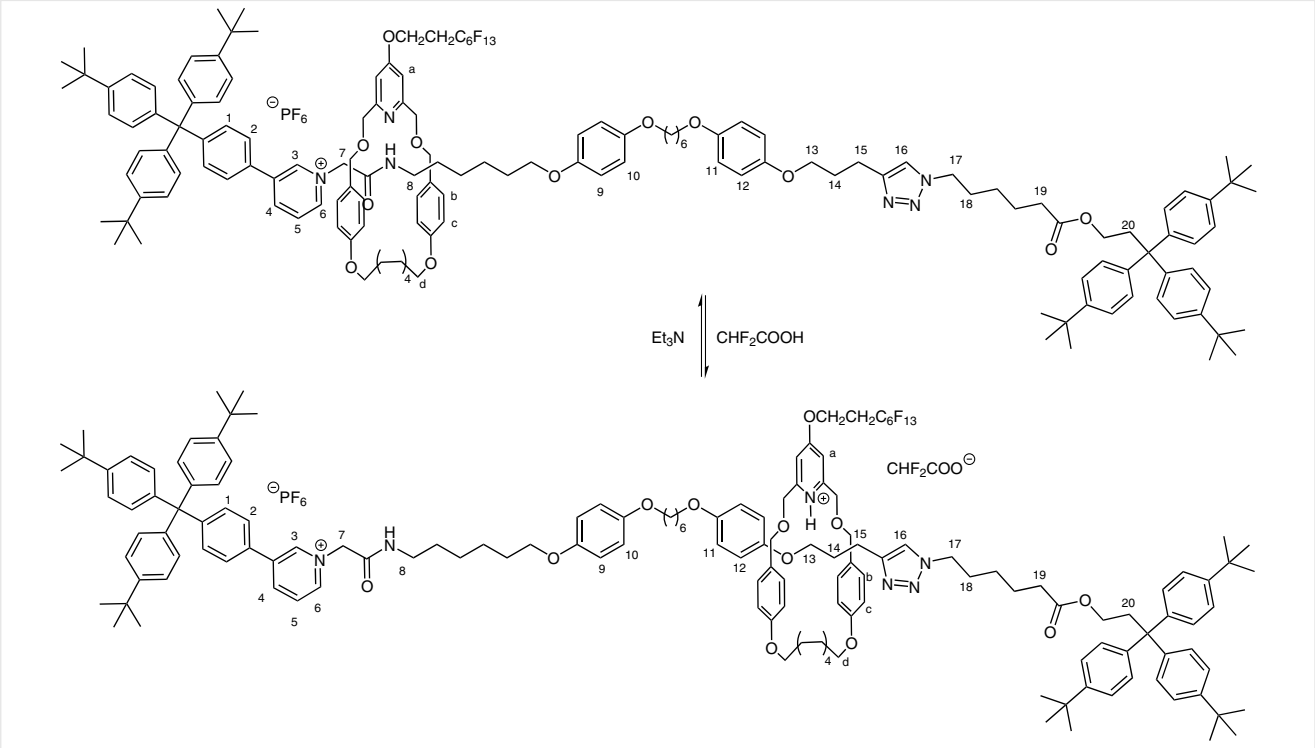

Scheme 4

The movement of the macrocyclic ring in rotaxane **12** as well as its new position on the axle could be identified by ^{1}H NMR spectra and 2D NOESY experiments. A downfield shift of the signals 1, 2, 4, 5, and 6 of the axle indicated that the protonated macrocycle is no longer next to the pyridinium ion. Instead, an upfield shift of the signals 11 to 15 was observed (Figure 3). This suggests that the macrocycle is predominantly located between the triazole ring and an adjacent aromatic ring (11, 12) (Scheme 4). This position may be preferred due to π–π-stacking of the aromatic rings or a hydrogen bond between the proton at the pyridine nitrogen atom of the macrocycle and a triazole nitrogen atom.

Neutralization with triethylamine led to deprotonation of the macrocycle and consequently, the macrocycle moved back to its original position next to the pyridinium ion (Scheme 4). The respective NMR spectrum showed that nearly all signals shifted back to their original position (Figure 3). Slight differences of some signals may be caused by an exchange of the counter ion in vicinity to the pyridinium unit. Besides the original hexafluorophosphate ion, now an excess of difluoracetate ions is present.

The main interest of this work was to optimize the workup and yield of the rotaxane synthesis from Hesseler.[8] A comparison of the yields of the nonfluorous rotaxane (7%) by Hesseler[8] with the fluorous rotaxane **12** (14%) showed that the yield could be doubled for the fluorous rotaxane **12**. It must be mentioned that the same workup and cleaning procedures were used. This leads to the conclusion that the fluorous ponytail has a huge impact on the chemical behavior of the rotaxane and thus on its separation and yield. Especially the difficult separation of the rotaxane from the free axle was simplified due to the fluorous ponytail. The fluorous rotaxane **12** shall show a faster mobility in chromatographies on silica gel. Indeed, this could be seen in TLC experiments. While the nonfluorous rotaxane possesses an R_f value of 0.13 on silica gel with dichloromethane–methanol (40:1) as eluent, the fluorous rotaxane **12** has an R_f value of 0.40. As a result, the separation from the free axle becomes easier.

To improve the separation even more, fluorous solid-phase extraction (FSPE) or column chromatography with fluorous silica gel might be helpful. In TLC experiments with fluorous silica gel, we observed a totally different behavior for the fluorous rotaxane **12** and the free axle but only if the hexafluorophosphate anion was exchanged against a nonfluorous anion like bromide. Due to strong interactions of the hexafluorophosphate anion with the fluorous silica gel, no retention was observed for the fluorous rotaxane **12** as well as for the free axle. The TLC experiments with bromide as counter ion are shown in Table 2.

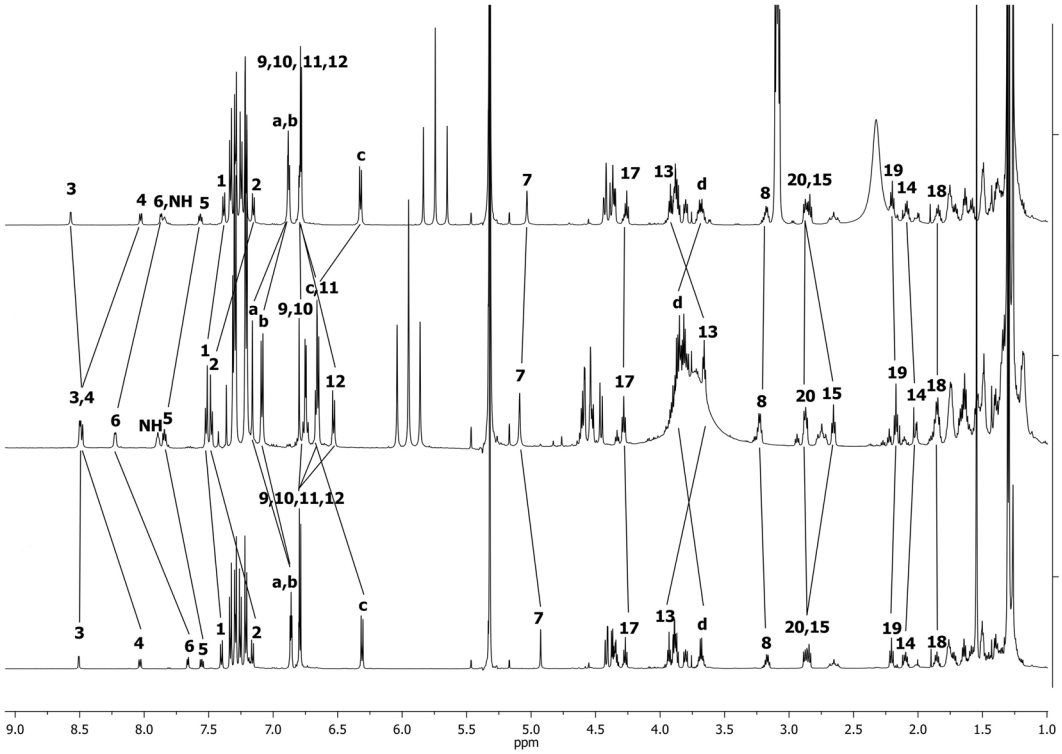

Figure 3 ^{1}H NMR spectra in CD_2Cl_2 of rotaxane **12** (bottom), rotaxane **12** after addition of 11 equiv of difluoroacetic acid (middle) and rotaxane **12** after neutralization with 11 equiv of triethylamine (top). Protons of the axle are numbered, protons of the ring are labeled with letters (see (Scheme 4). Chemically induced shifts are indicated by solid lines.

Table 2 TLC Experiments on Fluorous Silica Gel

Solvent	R_f		
	9	**13**	**12**
THF	1	1	1
MeOH	0.61	0.76	0.06
MeOH–H_2O (4:1)	0	0.63	0

A fluorophobic solvent mixture like methanol–water elutes the nonfluorous axle **13** only. By using more fluorophilic solvents like pure methanol or tetrahydrofuran, the fluorous macrocycle **9** as well as the fluorous rotaxane **12** could be eluted. This shows that the free axle might easily be separated by column chromatography with fluorous silica gel or even with fluorous solid-phase extraction. Nevertheless these experiments have shown the big potential of fluorous ponytails even for very large molecules like rotaxane **12**.

A protonable [2]rotaxane **12** was synthesized by the trapping method from a fluorous pyridine macrocycle **9**, an alkyne terminated half axle **10**, and a second azide terminated half axle **11** using the copper(I) catalyzed 1,3-dipolar cycloaddition ('click' reaction). Due to the fluorous ponytail, the separation of macrocyclic ring **9** and rotaxane **12** was possible by chromatography, and TLC studies showed that the use of fluorous stationary phases can simplify the workup even more. The properties of the isolated [2]rotaxane **12** were investigated by NMR spectroscopy and a shuttling process of the macrocyclic ring along the axle upon protonation/deprotonation could be verified.

All commercially available reagents were used without further purification. Anhydrous solvents were obtained with suitable desiccants. Chelidamic acid (**1**),[13,14] 4-hydroxypyridine-2,6-dicarboxylic acid diethyl ester (**2**),[17] 4-(hex-5-enyloxy)phenylmethanol (**6**),[15] (1-{2-oxo-2-[6-(4-{6-[4-(pent-4-ynyloxy)phenyloxy]hexyloxy}phenyloxy)hexyl]amino}ethyl)-3-{4-[tris(4-*tert*-butylphenyl)methyl]phenyl}pyridinium hexafluorophosphate (**10**),[8] and 6-azidohexanoic acid [3,3,3-tris(4-*tert*-butylphenyl)]propyl ester (**11**)[8] were prepared according to literature procedures. The behavior of rotaxane **12** on fluorous silica gel was checked by analytical TLC using FluoroFlash® F-254 precoated glass plates.

^{1}H and ^{13}C NMR spectra were recorded with Bruker DRX 500 and Bruker Avance 600 NMR spectrometers. For the numbering used to assign chemical shifts for the aromatic and pyridine rings of rotaxane **12** and axle **13**, please refer to the Supporting Information.

Mass spectra were recorded with Bruker-Daltronics Biflex III (MALDI), Bruker-Daltronics APEX 3 FT-ICR 7.05 T (ICR), and Jeol AccuTOF GCV 4G mass spectrometers. The matrix used for MALDI-TOF MS analysis is 4-chloro-α-cyanocinnamic acid (Cl-CCA).

4-[2-(Perfluorohexyl)ethyloxy]pyridine-2,6-dicarboxylic Acid Diethyl Ester (3)

A mixture of 4-hydroxypyridine-2,6-dicarboxylic acid diethyl ester (**2**; 5.03 g, 21.0 mmol) and Ag_2CO_3 (6.56 g, 23.8 mmol) in anhydrous toluene (350 mL) was stirred at 120 °C under N_2 for 2 h. Then, 1-iodo-2-(perfluorohexyl)ethane (7.68 mL, 31.4 mmol) was added dropwise and the reaction mixture was stirred for 3 d at 120 °C. Insoluble material was removed by filtration and washed with EtOAc (200 mL). The solvent was removed under reduced pressure and the crude product was purified by column chromatography (silica gel, CH_2Cl_2–EtOAc 15:1; R_f = 0.33) to give **3** as a colorless solid; yield: 11.4 g (93%); mp 70 °C.

IR (ATR): 2916, 2849 (aliph C–H), 1716 (C=O), 1600, 1584 (arom C=C), 1232, 1188 (C–O), 1143, 1118 (C–F), 1039 cm^{-1} (C–O).

^1H NMR (500 MHz, $CDCl_3$): δ = 7.79 (s, 2 H, PyH), 4.48 (q, ^3J = 7.1 Hz, 4 H, OCH_2CH_3), 4.45 (t, ^3J = 6.5 Hz, 2 H, OCH_2CH_2), 2.71 (t_Ft, $^3J_{H,F}$ = 18.0 Hz, ^3J = 6.5 Hz, 2 H, $OCH_2CH_2CF_2$), 1.45 (t, ^3J = 7.1 Hz, 6 H, OCH_2CH_3).

^{13}C NMR (125 MHz, $CDCl_3$): δ = 165.9 (s, 4-PyC), 164.5 (s, $PyCO_2Et$), 150.5 (s, 2,6-PyC), 117.3 (t_F, $^2J_{C,F}$ = 32.4 Hz, $CH_2CF_2CF_2$)*, 114.1 (d, 3,5-PyC), 62.5 (t, OCH_2CH_3), 60.9 (t, $OCH_2CH_2CF_2$), 31.0 [t(t_F), $^2J_{C,F}$ = 21.8 Hz, $CH_2CH_2CF_2$], 14.2 (q, OCH_2CH_3). * Only visible in the HMBC spectrum.

^{19}F NMR (470 MHz, $CDCl_3$): δ = –80.8 (s, 3 F, CF_3), –113.2 (s, 2 F, CH_2CF_2), –121.8 (s, 2 F, $CH_2CF_2CF_2$), –122.8 (s, 2 F, CF_2CF_3), –123.5 (s, 2 F, $CF_2CF_2CF_3$), –126.1 (s, 2 F, $CH_2CF_2CF_2CF_2$).

MS (EI): *m*/*z* = 586 $[M + H]^+$, 585 $[M]^{+\bullet}$, 584 $[M - H]^+$, 512 $[M - CO_2CH_2CH_3]^+$, 439 $[M - C_6H_{10}O_4]^+$.

HRMS (EI): *m*/*z* $[M]^{+\bullet}$ calcd for $C_{19}H_{16}F_{13}NO_5$: 585.0821; found: 585.0820.

2,6-Bis(hydroxymethyl)-4-[2-(perfluorohexyl)ethyloxy]pyridine (4)

$NaBH_4$ (675 mg, 17.8 mmol) was added to a solution of ethyl ester **3** (3.48 g, 5.95 mmol) in anhydrous THF (150 mL). The mixture was kept at 80 °C for 6 h. Afterwards, EtOH (50 mL) was added and the mixture was stirred for 12 h at r.t. The solvent was removed under reduced pressure and the residue was partitioned between EtOAc (100 mL) and H_2O (100 mL). The aqueous layer was extracted with EtOAc (3 × 150 mL), the combined organic layer was washed with brine (100 mL), and dried ($MgSO_4$). The solvent was removed under reduced pressure and **4** was obtained as a colorless solid; yield: 2.67 g (90%); mp 155 °C.

IR (ATR): 3300 (O–H), 1604, 1575 (arom C=C), 1237, 1191 (C–O), 1161, 1141 (C–F), 1090 cm^{-1} (C–O).

^1H NMR (500 MHz, $CDCl_3$): δ = 6.75 (s, 2 H, PyH), 4.72 (s, 4 H, $PyCH_2OH$), 4.35 (t, ^3J = 6.5 Hz, 2 H, OCH_2CH_2), 3.34 (br s, 2 H, OH), 2.66 (t_Ft, $^3J_{H,F}$ = 18.2 Hz, ^3J = 6.5 Hz, 2 H, $CH_2CH_2CF_2$).

^{13}C NMR (125 MHz, $CDCl_3$): δ = 165.7 (s, 4-PyC), 160.6 (s, 2,6-PyC), 117.1 (t_F, $CH_2CF_2CF_2$)*, 105.5 (d, 3,5-PyC), 64.3 (t, CH_2OH), 60.2 (t, $OCH_2CH_2CF_2$), 31.0 [t(t_F), $^2J_{C,F}$ = 21.9 Hz, $CH_2CH_2CF_2$]. * Only visible in the HMBC spectrum.

^{19}F NMR (470 MHz, $CDCl_3$): δ = –80.8 (s, 3 F, CF_3), –113.2 (s, 2 F, CH_2CF_2), –121.8 (s, 2 F, $CH_2CF_2CF_2$), –122.8 (s, 2 F, CF_2CF_3), –123.5 (s, 2 F, $CF_2CF_2CF_3$), –126.1 (s, 2 F, $CH_2CF_2CF_2CF_2$).

MS (EI): *m*/*z* = 502 $[M + H]^+$, 501 $[M]^{+\bullet}$, 500 $[M - H]^+$, 483 $[M - H_2O]^+$, 454 $[M - CH_4O_2]^+$.

HRMS (EI): *m*/*z* $[M]^{+\bullet}$ calcd for $C_{15}H_{12}F_{13}NO_5$: 501.0609; found: 501.0598.

2,6-Bis(bromomethyl)-4-[2-(perfluorohexyl)ethyloxy]pyridine (5)

PBr_3 (3.75 mL, 39.9 mmol) was added dropwise to a solution of alcohol **4** (2.00 g, 3.99 mmol) in $CHCl_3$ (150 mL). The mixture was stirred 6 h under reflux and afterwards 12 h at r.t. Sat. aq $NaHCO_3$ (150 mL) was added slowly and the mixture was stirred for 2 h at r.t. The aqueous phase was extracted with $CHCl_3$ (3 × 50 mL), the combined organic layer was washed with brine (100 mL), and dried ($MgSO_4$). The solvent was removed under reduced pressure and the crude product was purified by column chromatography (silica gel, *n*-heptane–EtOAc, 3:1; R_f = 0.30) to give **5** as a colorless solid; yield: 2.10 g (84%); mp 97 °C.

IR (ATR): 1597, 1571 (arom C=C), 1236, 1189 (C–O), 1165, 1141, 1122 (C–F), 1043 (C–O), 659 cm^{-1} (C–Br).

^1H NMR (500 MHz, $CDCl_3$): δ = 6.93 (s, 2 H, PyH), 4.52 (s, 4 H, $PyCH_2Br$), 4.37 (t, ^3J = 6.6 Hz, 2 H, OCH_2CH_2), 2.68 (t_Ft, $^3J_{H,F}$ = 18.2 Hz, ^3J = 6.6 Hz, 2 H, $CH_2CH_2CF_2$).

^{13}C NMR (125 MHz, $CDCl_3$): δ = 166.0 (s, 4-PyC), 158.3 (s, 2,6-PyC), 117.1 (t_F, $CH_2CF_2CF_2$)*, 109.3 (d, 3,5-PyC), 60.4 (t, $OCH_2CH_2CF_2$), 32.7 (t, CH_2Br) 31.0 [t(t_F), $^2J_{C,F}$ = 21.9 Hz, $CH_2CH_2CF_2$]. * Only visible in the HMBC spectrum.

^{19}F NMR (470 MHz, $CDCl_3$): δ = –80.8 (s, 3 F, CF_3), –113.2 (s, 2 F, CH_2CF_2), –121.8 (s, 2 F, $CH_2CF_2CF_2$), –122.8 (s, 2 F, CF_2CF_3), –123.5 (s, 2 F, $CF_2CF_2CF_3$), –126.1 (s, 2 F, $CH_2CF_2CF_2CF_2$).

MS (EI): *m*/*z* = 627 $[M + H]^+$, 626 $[M]^{+\bullet}$, 546 $[M - Br]^+$, 468 $[M + H - Br_2]^+$.

HRMS (EI): *m*/*z* $[M]^+$ calcd for $C_{15}H_{10}Br_2F_{13}NO$: 624.8921; found: 624.8934.

2,6-Bis[4-(hex-5-enyloxy)phenylmethyloxymethyl]-4-[2-(perfluorohexyl)ethyloxy)pyridine (7)

A solution of 4-(hex-5-enyloxy)phenylmethanol (**6**; 840 mg, 4.07 mmol) in anhydrous THF (30 mL) under N_2 was cooled to –78 °C. *i*-Pr_2NLi (2 M solution in THF, heptane, ethylbenzene, 2.04 mL, 4.07 mmol) was added dropwise and the mixture was stirred for 1 h at r.t. Afterwards, a solution of bromide **5** (730 mg, 1.16 mmol) in anhydrous THF (20 mL) was added, the mixture was heated slowly up to 50 °C, and then stirred for 3 d at 50 °C. After the addition of H_2O (50 mL), THF was removed under reduced pressure. The aqueous phase was extracted with CH_2Cl_2 (3 × 50 mL), the combined organic layer was washed with brine (100 mL), and dried ($MgSO_4$). The solvent was removed under reduced pressure and the crude product was purified by column chromatography (silica gel, *n*-heptane–EtOAc, 3:1; R_f = 0.14) to give **7** as a yellow oil; yield: 350 mg (34%).

IR (ATR): 2934, 2861 (aliph C-H), 1631 (C=C), 1600, 1582, 1512 (arom C=C), 1237, 1205 (C–O), 1162, 1144 (C–F), 1104 (C–O), 911 cm^{-1} (C=C–H).

^1H NMR (500 MHz, $CDCl_3$): δ = 7.30 (d, ^3J = 8.5 Hz, 4 H, 3,5-ArH), 6.94 (s, 2 H, 3,5-PyH), 6.88 (d, ^3J = 8.5 Hz, 4 H, 2,6-ArH), 5.83 (ddt, ^3J = 17.0 Hz, ^3J = 10.1 Hz, ^3J = 6.7 Hz, 2 H, CH_2CH=CH_2), 5.04 (dd, ^3J = 17.0 Hz, ^2J = 1.4 Hz, 2 H, CH=$CH H_{trans}$), 4.98 (d, ^3J = 10.1 Hz, 2 H, CH=$CH H_{cis}$), 4.62 (s, 4 H, Py-CH_2O), 4.58 (s, 4 H, ArCH_2O), 4.34 (t, ^3J = 6.5 Hz, 2 H, $PyOCH_2CH_2CF_2$), 3.96 (t, ^3J = 6.5 Hz, 4 H, $ArOCH_2$), 2.65 (m_c, 2 H, $CH_2CH_2CF_2$), 2.13 (m_c, 4 H, CH_2CH=CH_2), 1.80 (m_c, 4 H, OCH_2CH_2), 1.57 (m_c, 4 H, $OCH_2CH_2CH_2$).

^{13}C NMR (125 MHz, $CDCl_3$): δ = 166.0 (s, 4-PyC)*, 159.7 (s, 2,6-PyC) 158.8 (s, 1-ArC), 138.5 (d, *C*H=CH$_2$), 129.7 (s, 4-ArC), 129.6 (d, 3,5-ArC), 117.3 (t$_F$, *C*H$_2$CF$_2$CF$_2$)*, 114.7 (t, CH=*C*H$_2$), 114.5 (d, 2,6-ArC), 106.2 (d, 3,5-PyC), 72.8 (t, Ar*C*H$_2$O), 72.1 (t, Py*C*H$_2$O), 67.8 (t, ArO*C*H$_2$), 60.0 (t, PyO*C*H$_2$), 33.4 (t, *C*H$_2$CH=CH$_2$) 31.0 [t(t$_F$), $^2J_{C,F}$ = 21.5 Hz, CH$_2$*C*H$_2$CF$_2$], 28.7 (t, ArOCH$_2$*C*H$_2$), 25.3 (t, ArOCH$_2$CH$_2$*C*H$_2$). * Only visible in the HMBC spectrum.

^{19}F NMR (470 MHz, $CDCl_3$): δ = –80.8 (s, 3 F, CF_3), –113.2 (s, 2 F, CH_2CF_2), –121.8 (s, 2 F, $CH_2CF_2CF_2$), –122.8 (s, 2 F, CF_2CF_3), –123.5 (s, 2 F, $CF_2CF_2CF_3$), –126.1 (s, 2 F, $CH_2CF_2CF_2CF_2$).

MS (EI): *m*/*z* = 878 [M+H]$^+$, 877 [M]$^{+\bullet}$, 876 [M – H]$^+$, 673 [M + H – $C_{13}H_{17}O_2$]$^+$, 616 [M + H – $C_{17}H_{24}O_2$]$^+$, 590 [M + H – $C_{19}H_{28}O_2$]$^+$, 483 [M – $C_{26}H_{34}O_3$]$^+$, 468 [M + H – $C_{26}H_{34}O_4$]$^+$.

MS (MALDI-TOF, Cl-CCA): *m*/*z* = 900 [M + Na]$^+$, 878 [M + H]$^+$.

Anal. Calcd for $C_{41}H_{44}F_{13}NO_5$: C, 56.10; H, 5.05; N, 1.60. Found: C, 56.17; H, 4.75; N, 1.84.

5^4-[2-(Perfluorohexyl)ethyloxy]-3,7,10,21-tetraoxa-1,9(1,4)dibenzena-5(2,6)pyridinaheneicosaphan-15-ene (8)

A mixture of the macrocycle precursor **7** (300 mg, 342 µmol) and benzylidene-bis(tricyclohexylphosphine)dichlororuthenium (28.1 mg, 34.2 µmol) in anhydrous CH_2Cl_2 (350 mL) was stirred at r.t. under N_2 for 4 d. Afterwards, ethyl vinyl ether (1 mL) was added and the mixture was stirred for 1 h at r.t. The solvent was removed under reduced pressure and the crude product was purified by column chromatography (silica gel, CH_2Cl_2–EtOAc, 5:1, R_f = 0.20) to give **8** as a colorless solid; yield: 172 mg (59%). Product **8** is a mixture of *cis*- and *trans*-isomers (ratio 1:2).

trans-8

^{1}H NMR (500 MHz, $CDCl_3$): δ = 7.21 (d, ^3J = 8.5 Hz, 4 H, 3,5-ArH), 6.88 (s, 2 H, 3,5-PyH), 6.78 (d, ^3J = 8.5 Hz, 4 H, 2,6-ArH), 5.41 (m$_c$, 2 H, CH=CH), 4.58 (s, 4 H, Ar*CH*$_2$O), 4.39 (br s, 4 H, Py*CH*$_2$O), 4.36 (t, ^3J = 6.4 Hz, 2 H, PyOC*H*$_2$CH$_2$CF$_2$), 3.93 (t, ^3J = 6.7 Hz, 4 H, ArOC*H*$_2$), 2.66 (m$_c$, 2 H, CH$_2$*CH*$_2$CF$_2$), 2.02 (m$_c$, 4 H, *CH*$_2$CH=CHC*H*$_2$), 1.78–1.68 (m, 4 H, OCH$_2$C*H*$_2$), 1.54–1.44 (m, 4 H, OCH$_2$CH$_2$C*H*$_2$).

^{13}C NMR (125 MHz, $CDCl_3$): δ = 165.8 (s, 4-PyC)*, 159.9 (s, 2,6-PyC), 158.9 (s, 1-ArC), 130.4 (d, CH=CH), 130.1 (d, 3,5-ArC), 129.2 (s, 4-ArC), 117.3 (t$_F$, CH$_2$*C*F$_2$CF$_2$)*, 114.5 (d, 2,6-ArC), 106.3 (d, 3,5-PyC), 72.4 (t, Ar*C*H$_2$O), 71.1 (t, Py*C*H$_2$O), 67.6 (t, ArO*C*H$_2$), 60.0 (t, PyO*C*H$_2$), 31.9 (t, *C*H$_2$CH=CHC*H*$_2$), 31.1 [t(t$_F$), $^2J_{C,F}$ = 22.2 Hz, CH$_2$*C*H$_2$CF$_2$], 28.4 (t, OCH$_2$*C*H$_2$), 25.9 (t, OCH$_2$CH$_2$*C*H$_2$). * Only visible in the HMBC spectrum.

cis-8

IR (ATR): 2934, 2869 (aliph C–H), 1599, 1581, 1513 (arom C=C), 1237, 1193 (C–O), 1164, 1143, 1121 (C–F), 1061 cm^{-1} (C–O).

^{1}H NMR (500 MHz, $CDCl_3$): δ = 7.22 (d, ^3J = 8.5 Hz, 4 H, 3,5-ArH), 6.88 (s, 2 H, 3,5-PyH), 6.79 (d, ^3J = 8.5 Hz, 4 H, 2,6-ArH), 5.38 (m$_c$, 2 H, CH=CH), 4.57 (s, 4 H, Ar*CH*$_2$O), 4.44 (br s, 4 H, Py*CH*$_2$O), 4.36 (t, ^3J = 6.4 Hz, 2 H, PyOC*H*$_2$CH$_2$CF$_2$), 3.95 (t, ^3J = 6.7 Hz, 4 H, ArOC*H*$_2$), 2.66 (m$_c$, 2 H, CH$_2$*CH*$_2$CF$_2$), 2.06 (m$_c$, 4 H, *CH*$_2$CH=CHC*H*$_2$), 1.78–1.68 (m, 4 H, OCH$_2$C*H*$_2$), 1.54–1.44 (m, 4 H, OCH$_2$CH$_2$C*H*$_2$).

^{13}C NMR (125 MHz, $CDCl_3$): δ = 165.8 (s, 4-PyC)*, 159.9 (s, 2,6-PyC), 158.7 (s, 1-ArC), 130.1 (d, 3,5-ArC), 129.9 (d, CH=CH), 129.2 (s, 4-ArC), 117.3 (t$_F$, CH$_2$*C*F$_2$CF$_2$)*, 114.7 (d, 2,6-ArC), 106.3 (d, 3,5-PyC), 72.4 (t, Ar*C*H$_2$O), 71.1 (t, Py*C*H$_2$O), 67.5 (t, ArO*C*H$_2$), 60.0 (t, PyO*C*H$_2$), 31.1 [t(t$_F$), $^2J_{C,F}$ = 22.2 Hz, CH$_2$*C*H$_2$CF$_2$], 28.3 (t, OCH$_2$*C*H$_2$), 26.6 (t, *C*H$_2$CH=CHC*H*$_2$), 25.8 (t, OCH$_2$CH$_2$*C*H$_2$). * Only visible in the HMBC spectra.

^{19}F NMR (470 MHz, $CDCl_3$): δ = –80.8 (s, 3 F, CF_3), –113.2 (s, 2 F, CH_2CF_2), –121.8 (s, 2 F, $CH_2CF_2CF_2$), –122.8 (s, 2 F, CF_2CF_3), –123.5 (s, 2 F, $CF_2CF_2CF_3$), –126.1 (s, 2 F, $CH_2CF_2CF_2CF_2$).

MS (EI) : *m*/*z* = 850 [M + H]$^+$, 849 [M]$^{+\bullet}$, 848 [M – H]$^+$, 483 [M – $C_{18}H_{17}O_3$]$^+$, 469 [M + H – $C_{18}H_{17}O_4$]$^+$.

MS (MALDI-TOF, Cl-CCA): *m*/*z* = 872 [M + Na]$^+$, 850 [M + H]$^+$.

Anal. Calcd for $C_{39}H_{40}F_{13}NO_5$: C, 55.13; H, 4.74; N, 1.65. Found: C, 55.30; H, 4.25; N, 1.88.

5^4-[2-(Perfluorohexyl)ethyloxy]-3,7,10,21-tetraoxa-1,9-(1,4)-dibenzena-5-(2,6)-pyridinaheneicosaphane (9)

H_2 was bubbled through a suspension of PtO_2 (700 µg, 2.96 µmol) in acid-free $CHCl_3$ (3 mL) for 30 min. A solution of macrocycle **8** (28 mg, 33 µmol) in acid-free $CHCl_3$ (2 mL) was added, and the mixture was flushed with H_2 for further 2 h, followed by stirring for 3 d under H_2. The solvent was removed under reduced pressure and the crude product was purified by column chromatography (silica gel, CH_2Cl_2–EtOAc, 5:1, R_f = 0.54) to give **9** as a colorless solid; yield: 21 mg (75%); mp 85 °C.

IR (ATR): 2926, 2861 (aliph C–H), 1599, 1576, 1514 (arom C=C), 1240, 1195 (C–O), 1166, 1143, 1120 (C–F), 1061 cm^{-1} (C–O).

^{1}H NMR (500 MHz, $CDCl_3$): δ = 7.22 (d, ^3J = 8.6 Hz, 4 H, 3,5-ArH), 6.90 (s, 2 H, 3,5-PyH), 6.81 (d, ^3J = 8.6 Hz, 4 H, 2,6-ArH), 4.60 (s, 4 H, Ar*CH*$_2$O), 4.37 (br s, 4 H, Py*CH*$_2$O), 4.37 (t, ^3J = 6.5 Hz, 2 H, PyOC*H*$_2$CH$_2$CF$_2$), 3.97 (t, ^3J = 6.4 Hz, 4 H, ArOC*H*$_2$), 2.66 (m$_c$, 2 H, CH$_2$*CH*$_2$CF$_2$), 1.72 (m$_c$, 4 H, OCH$_2$C*H*$_2$), 1.45–1.37 (m, 4 H, OCH$_2$CH$_2$C*H*$_2$), 1.30–1.25 [m, 8 H, O(CH$_2$)$_3$C*H*$_2$CH$_2$].

^{13}C NMR (125 MHz, $CDCl_3$): δ = 165.6 (s, 4-PyC)*, 159.9 (s, 2,6-PyC) 158.8 (s, 1-ArC), 130.1 (d, 2,6-ArC), 129.1 (s, 4-ArC), 117.3 (t$_F$, CH$_2$*C*F$_2$CF$_2$)*, 114.6 (d, 3,5-ArC), 106.0 (d, 3,5-PyC), 72.4 (t, Ar*C*H$_2$O), 70.8 (t, Py*C*H$_2$O), 67.4 (t, ArO*C*H$_2$), 59.9 (t, PyO*C*H$_2$), 31.1 [t(t$_F$), $^2J_{C,F}$ = 22.0 Hz, CH$_2$*C*H$_2$CF$_2$], 29.5 [t, O(CH$_2$)$_4$*C*H$_2$], 28.7 [t, O(CH$_2$)$_3$*C*H$_2$], 28.6 (t, OCH$_2$*C*H$_2$), 25.7 (t, OCH$_2$CH$_2$*C*H$_2$). * Only visible in the HMBC spectrum.

^{19}F NMR (470 MHz, $CDCl_3$): δ = –80.8 (s, 3 F, CF_3), –113.2 (s, 2 F, CH_2CF_2), –121.8 (s, 2 F, $CH_2CF_2CF_2$), –122.8 (s, 2 F, CF_2CF_3), –123.5 (s, 2 F, $CF_2CF_2CF_3$), –126.1 (s, 2 F, $CH_2CF_2CF_2CF_2$).

MS (EI): *m*/*z* = 852 [M + H]$^+$, 851 [M]$^{+\bullet}$, 850 [M – H]$^+$, 483 [MH – $C_{24}H_{32}O_3$]$^+$, 469 [M – $C_{24}H_{30}O_4$]$^+$.

HRMS (EI): *m*/*z* [M]$^+$ calcd for $C_{39}H_{42}F_{13}NO_5$: 851.2855; found: 851.2832.

[2]-{[1-(2-Oxo-2-{[6-(4-{6-[4-(3-{1-[6-(3,3,3-tris{4-*tert*-butylphenyl}propyloxy)-6-oxohexyl]-1,2,3-triazole-4-yl}propyloxy)phenyloxy]hexyloxy}phenyloxy)hexyl]amino}ethyl)-3-{4-[tris(4-*tert*-butylphenyl)methyl]phenyl}pyridiniumhexafluorophosphate]-*rotaxa*-[5^4-(2-{perfluorohexyl}ethyloxy)-3,7,10,21-tetraoxa-1,9(1,4)dibenzena-5(2,6)pyridinaheneicosaphane]} (12)

To a mixture of macrocycle **9** (30.0 mg, 35.2 µmol), alkyne half axle **10** (42.9 mg, 35.2 µmol) and azide half axle **11** (21.0 mg, 35.2 µmol) in anhydrous CH_2Cl_2 (2 mL) under N_2 was added tetrakis(acetonitrile)copper(I) hexafluorophosphate (13.1 mg, 35.2 µmol). The mixture was stirred for 2 d at r.t. Afterwards, CH_2Cl_2 (4 mL) and MeOH (2 mL) were added to dilute the mixture. KCN (11.5 mg, 176 µmol) in MeOH (2 mL) was added and the mixture was stirred for 1 h. The solvent was removed under reduced pressure and the crude product was partitioned between CH_2Cl_2 (10 mL) and H_2O (10 mL). The aqueous phase was extracted with CH_2Cl_2 (3 × 10 mL), the combined organic layer was washed with brine (20 mL), and dried ($MgSO_4$). The solvent

was removed under reduced pressure and the crude product was purified by column chromatography (silica gel, CH_2Cl_2–MeOH, 40:1; R_f = 0.40) to give **12** as yellow solid; yield: 13 mg (14%). Additionally, the free axle **13** was isolated; yield: 31 mg (48%).

Rotaxane 12

^{1}H NMR (600 MHz, CD_2Cl_2): δ = 8.49 (s, 1 H, 2-Py^{1}H), 8.04 (d, ^3J = 8.1 Hz, 1 H, 4-Py^{1}H), 7.65 (d, ^3J = 6.2 Hz, 1 H, 6-Py^{1}H), 7.55 (dd, ^3J = 8.1 Hz, ^3J = 6.2 Hz, 1 H, 5-Py^{1}H), 7.40 (d, ^3J = 8.5 Hz, 2 H, 3,5-Ar^{2}H), 7.33 (d, ^3J = 8.7 Hz, 6 H, 3,5-Ar^{1}H), 7.31–7.28 (m, 7 H, 5-triazole-H, 3,5-Ar^{5}H), 7.25 (d, ^3J = 8.7 Hz, 6 H, 2,6-Ar^{1}H), 7.23–7.20 (m, 7 H, CONH, 2,6-Ar^{5}H), 7.16 (d, ^3J = 8.5 Hz, 2 H, 2,6-Ar^{2}H), 6.86 (d, ^3J = 8.6 Hz, 4 H, 3,5-Ar^{6}H), 6.86 (s, 2 H, 3,5-Py^{2}H), 6.79 (d, ^3J = 6.3 Hz, 8 H, 2,3,5,6-Ar^{3}H, 2,3,5,6-Ar^{4}H), 6.31 (d, ^3J = 8.6 Hz, 4 H, 2,6-Ar^{6}H), 4.92 (s, 2 H, Py^{1}CH_2CONH), 4.43–4.32 (m, 10 H, Py^{2}CH_2O, Ar^{6}CH_2O, Py^{2}OCH_2), 4.27 [t, ^3J = 7.2 Hz, 2 H, triazole-CH_2(CH$_2$)$_4$CO$_2$], 3.93 [t, ^3J = 6.2 Hz, 2 H, Ar^{4}OCH_2(CH$_2$)$_2$-triazole], 3.91–3.85 [m, 6 H, CH_2OAr^{3}OCH_2(CH$_2$)$_4$CH_2OAr^4], 3.80 (m$_c$, 2 H, CO$_2$CH_2CH$_2$), 3.72–3.64 (m$_c$, 4 H, Ar^{6}OCH_2), 3.20–3.14 (m, 2 H, NHCH_2), 2.91–2.81 [m, 4 H, Ar^{4}O(CH$_2$)$_2$CH_2-triazole, CO$_2$CH$_2$CH_2], 2.65 (m$_c$, 2 H, OCH$_2$CH_2CF$_2$), 2.21 [t, ^3J = 7.6 Hz, 2 H, triazole-(CH$_2$)$_4$CH_2CO$_2$], 2.10 (m$_c$, 2 H, Ar^{4}OCH$_2$CH_2CH$_2$-triazole), 1.85 [m$_c$, 2 H, triazole-CH$_2$CH_2(CH$_2$)$_3$CO$_2$], 1.80–1.69 [m, 6 H, CH_2CH$_2$OAr^{3}OCH$_2$CH_2(CH$_2$)$_2$CH_2CH$_2$OAr^4], 1.67–1.61 (m, 4 H, Ar^{6}OCH$_2$CH_2), 1.61–1.56 [m, 2 H, triazole-(CH$_2$)$_3$CH_2CH$_2$CO$_2$], 1.52–1.48 [m, 6 H, NHCH$_2$CH_2, Ar^{3}O(CH$_2$)$_2$CH_2CH_2(CH$_2$)$_2$OAr^4], 1.47–1.44 [m, 2 H, NH(CH$_2$)$_3$CH_2(CH$_2$)$_2$OAr^3], 1.41–1.38 [m, 4 H, Ar^{6}O(CH$_2$)$_2$CH_2], 1.37–1.34 [m, 2 H, NH(CH$_2$)$_2$CH_2(CH$_2$)$_3$OAr^3], 1.34–1.22 [m, 10 H, Ar^{6}O(CH$_2$)$_3$CH_2CH_2, triazole-(CH$_2$)$_2$CH_2(CH$_2$)$_2$CO$_2$], 1.30, 1.29 [2 s, 54 H, 6 × C(CH$_3$)$_3$].

^{13}C NMR (150 MHz, CD_2Cl_2): δ = 173.8 (s, CO$_2$CH$_2$), 166.3 (s, 4-Py^{2}C), 163.4 (s, CONH)*, 159.7 (s, 2,6-Py^{2}C), 159.2 (s, 1-Ar^{6}C), 153.9, 153.8, 153.7, 153.6 (4 s, 1,4-Ar^{3}C, 1,4-Ar^{4}C), 151.1 (s, 4-Ar^{2}C)*, 149.5 (s, 4-Ar^{1}C), 149.4 (s, 4-Ar^{5}C), 147.7 (s, 4-triazole-C), 144.7 (d, 2-Py^{1}C),144.5 (s, 1-Ar^{5}C), 144.3 (s, 1-Ar^{1}C), 142.8 (d, 6-Py^{1}C), 141.6 (d, 4-Py^{1}C), 140.3 (s, 3-Py^{1}C), 132.2 (d, 3,5-Ar^{2}C), 130.9 (d, 2,6-Ar^{1}C), 130.7 (d, 3,5-Ar^{6}C), 129.5 (s, 1-Ar^{2}C), 129.3 (s, 4-Ar^{6}C)*, 129.0 (d, 2,6-Ar^{5}C), 126.9 (d, 2,6-Ar^{2}C), 126.6 (s, 5-Py^{1}C), 125.4 (d, 3,5-Ar^{5}C), 125.3 (d, 3,5-Ar^{1}C), 121.3 (d, 5-triazole-C), 118.3 (t$_F$, Py^{2}OCH$_2$CH$_2$CF$_2$), 115.8 (d, 2,3,5,6-Ar^{3}C, 2,3,5,6-Ar^{4}C), 114.6 (d, 2,6-Ar^{6}C), 108.7 (d, 3,5-Py^{2}C), 73.8 (t, Ar^{6}CH$_2$O), 73.4 (t, Py^{2}CH$_2$O), 69.0, 68.9 [t, CH$_2$OAr^{3}OCH$_2$(CH$_2$)$_4$CH$_2$OAr^4], 68.1 (t, Ar^{4}OCH$_2$CH$_2$CH$_2$-triazole), 67.8 (t, Ar^{6}OCH$_2$), 64.5 [s, C(Ar^1)$_3$], 63.0 (t, CO$_2$CH$_2$CH$_2$), 62.2 (t, Py^{1}CH$_2$), 60.9 (t, Py^{2}OCH$_2$CH$_2$CF$_2$), 54.1 [s, C(Ar^5)$_3$], 50.4 [t, triazole-CH$_2$(CH$_2$)$_4$CO$_2$], 40.7 (t, NHCH$_2$), 38.8 (t, CO$_2$CH$_2$CH$_2$), 34.8, 34.8 [2 s, Ar^{1}C(CH$_3$)$_3$, Ar^{5}C(CH$_3$)$_3$], 34.4 (t, CH$_2$CO$_2$), 31.6 [q, Ar^{1}C(CH$_3$)$_3$, Ar^{5}C(CH$_3$)$_3$], 31.5 (t, Py^{2}OCH$_2$CH$_2$CF$_2$), 30.6 [t, triazole-CH$_2$CH$_2$(CH$_2$)$_3$CO$_2$], 29.9, 29.8 [2 t, OAr^{3}OCH$_2$CH$_2$(CH$_2$)$_2$CH$_2$CH$_2$OAr^4], 29.7 (t, Ar^{4}OCH$_2$CH$_2$CH$_2$-triazole), 29.6 [t, NH(CH$_2$)$_4$CH$_2$CH$_2$OAr^3], 29.5 (t, NHCH$_2$CH$_2$), 29.2 [t(t$_F$), Ar^{6}OCH$_2$CH$_2$], 27.2 [t, NH(CH$_2$)$_2$CH$_2$(CH$_2$)$_3$OAr^3], 26.5 [t, Ar^{6}O(CH$_2$)$_3$CH$_2$CH$_2$], 26.4, 26.4 [2 t, NH(CH$_2$)$_3$CH$_2$(CH$_2$)$_2$OAr^3, Ar^{3}O(CH$_2$)$_2$CH$_2$CH$_2$(CH$_2$)$_2$OAr^4], 26.3 [t, Ar^{6}O(CH$_2$)$_2$CH$_2$], 24.8 [t, triazole-(CH$_2$)$_3$CH$_2$CH$_2$CO$_2$], 23.3 [t, triazole-(CH$_2$)$_2$CH$_2$(CH$_2$)$_2$CO$_2$], 22.7 (t, Ar^{4}OCH$_2$CH$_2$CH$_2$triazole). * Only visible in the HMBC spectra.

^{19}F NMR (470 MHz, CD_2Cl_2): δ = –72.6 (d, ^1J_P = 711 Hz, 6 F, PF$_6$), –81.1 (s, 3 F, CF$_3$), –113.5 (s, 2 F, CH$_2$CF$_2$), –122.0 (s, 2 F, CH$_2$CF$_2$CF$_2$), –123.0 (s, 2 F, CF$_2$CF$_3$), –123.7 (s, 2 F, CF$_2$CF$_2$CF$_3$), –126.3 (s, 2 F, CH$_2$CF$_2$CF$_2$CF$_2$).

MS (MALDI-TOF, Cl-CCA): m/z = 2522 [M – PF$_6$]$^+$.

HRMS (FT-ICR, CH_2Cl_2–MeOH): m/z [M – PF$_6$ + H]$^{2+}$ calcd for $C_{151}H_{184}F_{13}N_6O_{12}^{2+}$: 1260.691; found: 1260.698.

Axle 13

^{1}H NMR (600 MHz, CD_2Cl_2): δ = 9.49 (s, 1 H, 2-PyH), 9.01 (br s, 1 H, CONH), 8.99 (d, ^3J = 6.1 Hz, 1 H, 6-PyH), 8.57 (d, ^3J = 8.2 Hz, 1 H, 4-PyH), 7.98 (dd, ^3J = 8.2 Hz, ^3J = 6.1 Hz, 1 H, 5-PyH), 7.63 (d, ^3J = 8.6 Hz, 2 H, 2,6-Ar^{2}H), 7.53 (d, ^3J = 8.6 Hz, 2 H, 3,5-Ar^{2}H), 7.36–7.24 (m, 13 H, 3,5-Ar^{5}H, 3,5-Ar^{1}H, 5-triazole-H), 7.24–7.17 (m, 12 H, 2,6-Ar^{5}H, 2,6-Ar^{1}H), 6.80, 6.78 (2 s, 8 H, 2,3,5,6-Ar^{3}H, 2,3,5,6-Ar^{4}H), 5.68 (s, 2 H, Py^{1}CH_2CONH), 4.28 [t, ^3J = 7.2 Hz, 2 H, triazole-CH_2(CH$_2$)$_4$CO$_2$], 3.94 [t, ^3J = 6.2 Hz, 2 H, Ar^{4}OCH_2(CH$_2$)$_2$-triazole], 3.91–3.88 [m, 4 H, Ar^{3}OCH_2(CH$_2$)$_4$CH_2OAr^4], 3.86 [t, ^3J = 6.5 Hz, 2 H, NH(CH$_2$)$_5$CH_2OAr^3], 3.81 (m$_c$, 2 H, CO$_2$CH_2CH$_2$), 3.25 (m$_c$, 2 H, NHCH_2CH$_2$), 2.91–2.83 [m, 4 H, Ar^{4}O(CH$_2$)$_2$CH_2-triazole, CO$_2$CH$_2$CH_2], 2.21 [t, ^3J = 7.5 Hz, 2 H, triazole-(CH$_2$)$_4$CH_2CO$_2$], 2.10 (m$_c$, 2 H, Ar^{4}OCH$_2$CH_2CH$_2$-triazole), 1.87 [m$_c$, 2 H, triazole-CH$_2$CH_2(CH$_2$)$_3$CO$_2$], 1.82–1.68 [m, 6 H, CH_2CH$_2$OAr^{3}OCH$_2$CH_2(CH$_2$)$_2$CH_2CH$_2$OAr^4], 1.67–1.55 [m, 4 H, triazole-(CH$_2$)$_3$CH_2CH$_2$CO$_2$, NHCH$_2$CH_2], 1.54–1.47 [m, 8 H, NH(CH$_2$)$_2$CH_2CH$_2$(CH$_2$)$_2$OAr^{3}O(CH$_2$)$_2$CH_2CH$_2$(CH$_2$)$_2$OAr^4], 1.46–1.37 [m, 2 H, triazole-(CH$_2$)$_2$CH_2(CH$_2$)$_2$CO$_2$], 1.31, 1.30 [2 s, 54 H, 6 × C(CH$_3$)$_3$].

^{13}C NMR (150 MHz, CD_2Cl_2): δ = 173.8 (s, CO$_2$CH$_2$), 164.2 (s, CONH), 153.9, 153.8, 153.7, 153.6 (4 s, 1,4-Ar^{3}C, 1,4-Ar^{4}C), 151.4 (s, 4-Ar^{2}C)*, 149.5 (s, 4-Ar^{5}C), 149.4 (s, 4-Ar^{1}C), 147.7 (s, 4-triazole-C), 144.5 (s, 1-Ar^{5}C), 144.1 (s, 1-Ar^{1}C), 143.9 (d, 2-PyC), 143.5 (d, 6-PyC), 143.2 (d, 4-PyC), 141.5 (s, 3-PyC)*, 133.0 (d, 3,5-Ar^{2}C), 131.0 (d, 2,6-Ar^{1}C), 130.3 (s, 1-Ar^{2}C), 129.0 (d, 2,6-Ar^{5}C), 128.2 (d, 5-PyC), 127.0 (d, 2,6-Ar^{2}C), 125.4 (d, 3,5-Ar^{1}C), 125.2 (d, 3,5-Ar^{5}C), 121.3 (d, 5-triazole-C), 115.9 (d, 2,3,5,6-Ar^{3}C, 2,3,5,6-Ar^{4}C), 69.1 [t, CH$_2$OAr^{3}OCH$_2$(CH$_2$)$_4$CH$_2$OAr^4], 68.1 (t, Ar^{4}OCH$_2$CH$_2$CH$_2$-triazole), 64.6 [s, C(Ar^1)$_3$], 63.1 (t, PyCH$_2$), 63.0 (t, CO$_2$CH$_2$CH$_2$), 54.1 [s, C(Ar^5)$_3$], 50.4 [t, triazole-CH$_2$(CH$_2$)$_4$CO$_2$], 40.7 (t, NHCH$_2$), 38.8 (t, CO$_2$CH$_2$CH$_2$), 34.8, 34.8 [2 s, Ar^{1}C(CH$_3$)$_3$, Ar^{5}C(CH$_3$)$_3$], 34.4 (t, CH$_2$CO$_2$), 31.6 [q, Ar^{1}C(CH$_3$)$_3$, Ar^{5}C(CH$_3$)$_3$], 30.6 [t, triazole-CH$_2$CH$_2$(CH$_2$)$_3$CO$_2$], 29.9, 29.8, 29.7 [3 t, CH$_2$CH$_2$OAr^{3}OCH$_2$CH$_2$(CH$_2$)$_2$CH$_2$CH$_2$OAr^4], 29.5 (t, Ar^{4}OCH$_2$CH$_2$CH$_2$-triazole), 29.2 (t, NHCH$_2$CH$_2$), 26.6 [t, NH(CH$_2$)$_3$CH$_2$(CH$_2$)$_2$OAr^3], 26.4 [t, Ar^{3}O(CH$_2$)$_2$CH$_2$CH$_2$(CH$_2$)$_2$OAr^4], 26.3 [t, triazole-(CH$_2$)$_2$CH$_2$(CH$_2$)$_2$CO$_2$], 26.2 [t, NH(CH$_2$)$_2$CH$_2$(CH$_2$)$_3$OAr^3], 24.8 [t, triazole-(CH$_2$)$_3$CH$_2$CH$_2$CO$_2$], 22.7 (t, Ar^{4}OCH$_2$CH$_2$CH$_2$-triazole). * Only visible in the HMBC spectra.

MS (MALDI-TOF, Cl-CCA): m/z = 1670 [M – PF$_6$]$^+$.

Acknowledgment

The support of the Deutsche Forschungsgemeinschaft (SFB 677) is greatfully acknowledged.

Supporting Information

Supporting information for this article is available online at http://dx.doi.org/10.1055/s-0034-1380814.

References

(1) Boyer, P. D. *Biochim. Biophys. Acta (Bioenergetics)* **1993**, *1140*, 215.
(2) Baudry, J.; Tajkhorshid, E.; Molnar, F.; Phillips, J.; Schulten, J. *J. Phys. Chem. B* **2001**, *105*, 905.
(3) (a) *Molecular Machines and Motors*, In *Topics in Current Chemistry*; Vol. 354; Credi, A.; Silvi, S.; Venturi, M., Eds.; Springer-Verlag: Berlin, **2014**. (b) Balzani, V.; Credi, A.; Venturi, M. *Molecular Devices and Machines - Concepts and Perspectives for the Nanoworld*, 2nd ed.; Wiley-VCH: Weinheim, **2008**. (c) *Molecular*

Switches, 2nd ed.; Feringa, B. L.; Browne, W. R., Eds.; Wiley-VCH: Weinheim, **2011**. (d) *Molecular Machines*, In *Topics in Current Chemistry*; Vol. 262; Kelly, T., Ed.; Springer-Verlag: Berlin, **2005**.
(4) Schwörer, M.; Wirz, J. *Helv. Chim. Acta* **2001**, *84*, 1441; and references cited therein.
(5) Frej, A.; Goeschen, C.; Näther, C.; Lüning, U.; Herges, R. *J. Phys. Org. Chem.* **2010**, *23*, 1093.
(6) Some reviews on MIMs: (a) *Molecular Catenanes, Rotaxanes and Knots – A Journey Through the World of Molecular Topology*; Sauvage, J.-P.; Dietrich-Buchecker, C., Eds.; Wiley-VCH: Weinheim, **1999**. (b) Stoddart, J. F. *Angew. Chem. Int. Ed.* **2014**, *53*, 11102; *Angew. Chem.* **2014**, *126*, 11282. (c) Ayme, J.-F.; Beves, J. E.; Campbell, C. J.; Leigh, D. A. *Chem. Soc. Rev.* **2013**, *42*, 1700; and references cited therein.
(7) (a) Vetter, W.; Schill, G. *Tetrahedron* **1967**, *23*, 3079. (b) Schill, G. *Catenanes, Rotaxanes, and Knots*; Academic Press: New York, **1971**. (c) Schalley, C. A.; Beizai, K.; Vögtle, F. *Acc. Chem. Res.* **2001**, *34*, 465. (d) Bruns, C. J.; Stoddart, J. F. *Acc. Chem. Res.* **2014**, *47*, 2186.
(8) Hesseler, B.; Zindler, M.; Herges, R.; Lüning, U. *Eur. J. Org. Chem.* **2014**, 3885.
(9) Aucagne, V.; Hänni, K. D.; Leigh, D. A.; Lusby, P. J.; Walker, D. B. *J. Am. Chem. Soc.* **2006**, *128*, 2186.
(10) (a) Hesseler, B. *Ph.D. Thesis*; Christian-Albrechts-Universität zu Kiel: Germany, **2014**. (b) Zindler, M. *Ph. D. Thesis*; Christian-Albrechts-Universität zu Kiel: Germany, **2012**.
(11) *Handbook of Fluorous Chemistry*; Gladysz, J. A.; Curran, D. P.; Horváth, I. T., Eds.; Wiley-VCH: Weinheim, **2004**.
(12) (a) Eckelmann, J.; Lüning, U. *Chem. Unserer Zeit* **2009**, *43*, 210. (b) Eckelmann, J.; Lüning, U. *J. Chem. Educ.* **2013**, *90*, 224.
(13) Horvath, G.; Rusa, C.; Köntös, Z.; Gerencser, J.; Huszthy, P. *Synth. Commun.* **1999**, *29*, 3719.
(14) Chauvin, A.-S.; Comby, S.; Song, B.; Vandevyver, C. D. B.; Bünzli, J.-C. G. *Chem. Eur. J.* **2008**, *14*, 1726.
(15) Mak, E.; Zindler, M.; Hartkopf, B.; Herges, R.; Lüning, U. *Eur. J. Org. Chem.* **2010**, 4932.
(16) Aucagne, V.; Berná, J.; Crowley, J. D.; Goldup, S. M.; Hänni, K. D.; Lusby, P. J.; Ronaldson, V. E.; Slawin, A. M.; Viterisi, A.; Walker, D. B.; Leigh, D. A. *J. Am. Chem. Soc.* **2007**, *129*, 11950.
(17) Lamture, J. B.; Zhou, Z. H.; Kumar, A. S.; Wensel, T. G. *Inorg. Chem.* **1995**, *34*, 864.